Journal of Applied Fluid Mechanics, Vol. 9, No. 5, pp. 2277-2289, 2016.
Available online at www.jafmonline.net, ISSN 1735-3572, EISSN 1735-3645.
DOI: 10.18869/acadpub.jafm.68.236.25641

Mixed Convection of Alumina/Water Nanofluid in Microchannels using Modified Buongiorno's Model in Presence of Heat Source/Sink

A. Malvandi[1†] and D. D. Ganji[2]

[1] *Young Researchers and Elite Club, Karaj Branch, Islamic Azad University, Karaj, Iran*
[2] *Mechanical Engineering Department, Babol University of Technology, Babol, Iran*

†*Corresponding Author Email: amirmalvandi@aut.ac.ir*

(Received September 24, 2015; accepted November 8, 2015)

ABSTRACT

The nanoparticle migration effects on mixed convection of alumina/water nanofluid in a vertical microchannel in the presence of heat source/sink with asymmetric wall heating are theoretically investigated. The modified two-component heterogeneous model is employed for the nanofluid in the hypothesis that the Brownian motion and the thermophoresis are the only significant bases of nanoparticle migration. Because of low dimensional structures in microchannels, a linear slip condition is considered at the surfaces, which appropriately represents the non-equilibrium region near the interface. Considering hydrodynamically and thermally fully developed flow, the basic partial differential equations including the continuity, momentum, energy, and nanoparticle fraction have been reduced to two-point ordinary boundary value differential equations before they have been solved numerically. The scale analysis of governing equations has shown that the buoyancy effects due to the temperature distribution is insignificant, however, the buoyancy effects due to the concentration distribution of nanoparticles have considerable effects on the flow and heat transfer characteristics of nanofluids. It is also revealed that the imposed thermal asymmetry would change the direction of nanoparticle migration and distorts the symmetry of the velocity, temperature and nanoparticle concentration profiles. Moreover, the best performance of the system is achieved under one-sided heating and a greater slip velocity at the walls.

Keywords: Nanofluid; Nanoparticles migration; Mixed convection; Thermal asymmetry; Microchannel; Modified Buongiorno's Model.

NOMENCLATURE

c_p	specific heat at constant pressure	Nu	Nusselt number
D_B	Brownian diffusion coefficient	N_{BT}	ratio of the Brownian to thermophoretic
D_T	thermophoresis diffusion coefficient	p	pressure
h	heat transfer coefficient	Iq_w	surface heat flux
H	half of height of the channel	T	temperature
k	thermal conductivity	φ	nanoparticle volume fraction
k_{BO}	Boltzmann constant	$\gamma\rho$	density

1. INTRODUCTION

Economic incentives, energy saving and space considerations have increased efforts to construct a more efficient heat exchange equipment. In modern industrial applications, conventional techniques are not appropriate any longer and heat transfer enhancement methods are of main concerns of scientists. Generally, enhancement techniques can be divided into two groups: a) passive techniques which require special surface geometries Nobari and Malvandi (2013) , thermal packaging or fluid additives, and b) active techniques which require external forces such as an electrical and magnetic forces. The active techniques need additional power that increases initial capital and operational costs of the system, although they commonly present a higher augmentation. In contrast, the passive techniques do not require any direct input of external power; so, they hold the advantage over the

active techniques. These techniques generally use surface or geometrical modifications such microchannels or altering the working fluid such as Newtonian or non-Newtonian fluids. Usually channels with a hydraulic diameter below 5mm are categorized as microchannels that are widely used in efficient new cooling systems such as electronic devices, automobile cooling systems and heat pipes.

The idea behind the fluid additives is to improve the thermal conductivity of the most common fluids such as water, oil, and ethylene-glycol mixture, which is emerged by Maxwell (1873). Later, many researchers studied the influence of solid-liquid mixtures on potential heat transfer enhancement. However, they were confronted with problems such as abrasion, clogging, fouling and additional pressure loss of the system which makes these unsuitable for heat transfer systems. In 1995, the word "nanofluid" was proposed by Choi (1995) to indicate dilute suspensions formed by functionalized nanoparticles smaller than 100nm in diameter which had already been created by Masuda *et al*. (1993) as Al_2O_3-water. These nanoparticles are fairly close in size to the molecules of the base fluid and, thus, can enable extremely stable suspensions with only slight gravitational settling over long periods.

Aligned with the same proposition, theoretical studies emerged to model the nanofluid behaviors. There were commonly two models to develop the mathematical model for transport behavior of nanofluids; one is single component (homogeneous) model where the thermophysical properties of base fluid are modified with the nanoparticle influenced correlations of viscosity and thermal conductivity and another is two component (non-homogeneous) model, explained by Buongiorno (2006) which consists of two slip mechanisms; Brownian diffusion and thermophoresis. Some recent investigations show the transport process in nanofluid with different physical occurring situations by considering single as well as two component model. Buongiorno (2006) demonstrated that the homogeneous models tend to underpredict the nanofluid heat transfer coefficient, whereas the dispersion effect is completely negligible due to the nanoparticle size. Hence, Buongiorno developed an alternative model to explain the anomalous convective heat transfer in nanofluids and so eliminate the shortcomings of the homogeneous and dispersion models. He asserted that the anomalous heat transfer occurs due to particle migration in the fluid. Investigating the nanoparticle migration, he considered seven slip mechanisms — the inertia, Brownian diffusion, thermophoresis, diffusiophoresis, Magnus forces, fluid drainage, and gravity — and maintained that, of these seven, only Brownian diffusion and thermophoresis are important slip mechanisms in nanofluids. Taking this finding as a basis, he proposed a two-component four-equation non-homogeneous equilibrium model for convective transport in nanofluids. The model has been used by Kuznetsov and Nield (2010) to study the influence of nanoparticles on the natural convection boundary-layer flow past a vertical plate, Tzou (2008) for the analysis of nanofluid Bernard convection, Hwang *et al*. (2009) for the analysis of laminar forced convection. Then, a comprehensive survey of convective transport of nanofluids were conducted by Soleimani *et al*. (2012), Sheikholeslami *et al*. (2013), Sheikholeslami *et al*. (2013), Sheikholeslami *et al*. (2014), Rashidi *et al*. (2014), Rashidi *et al*. (2014), Mahmoodi and Hashemi (2012), Yadav *et al*. (2012), Yadav *et al*. (2013), Yadav *et al*. (2015), Shamshirband *et al*. (2015), Malvandi *et al*. (2014), Malvandi *et al*. (2014), and Ashorynejad *et al*. (2013).

Recently, Buongiorno's model has been modified by Yang *et al*. (2013) to fully account for the effects of the nanoparticle volume fraction. Malvandi *et al*. (2014), then, extended their study to consider the mutual effects of buoyancy and nanoparticle migration for mixed convection of nanofluids in vertical annular tubes. In another study, Malvandi and Ganji (2014) studied the impacts of nanoparticle migration on alumina/water nanofluids in a parallel-plate channel. They indicated that the motion of nanoparticles is from the adiabatic wall (nanoparticle depletion) to the cold wall (nanoparticle accumulation) which it leads to construction a non-uniform nanoparticle distribution. Later, the modified Buongiorno's model has been applied to different heat transfer concepts including forced Malvandi and Ganji (2014), Malvandi *et al*. (2014),Moshizi *et al*. (2014), mixed (Ganji and Malvandi (2014), Malvandi and Ganji (2014), Malvandi *et al*. (2014)), and natural convection (Ganji and Malvandi (2014)). Recently, Hedayati and Domairry (2015) have analyzed the effect of nanoparticles migration and asymmetric heating on mixed convection of TiO_2-H_2O nanofluid inside a vertical microchannel. The results indicated that the modified model is an appropriate model for considering the effects of nanoparticle migration in nanofluids.

In this paper, the laminar fully developed mixed convection of alumina/water nanofluid inside a vertical microchannel in presence of heat source/sink is investigated theoretically using the modified two-component heterogeneous model of Buongiorno Yang *et al*. (2013), Malvandi *et al*. (2014). Because of low dimensional structures in microchannels, a linear slip condition Malvandi *et al*. (2014) is considered at the surfaces, which appropriately represents the non-equilibrium region near the interface. The parallel flat surfaces making the microchannel boundaries were kept at constant but different heat fluxes. The thermal asymmetry thus imposed on the system changes the mechanism of nanoparticle migration which is one of the main motivations of this study. Note that the current study can be considered as an extended version of the authors' previous work Malvandi *et al*. (2014), where the scale analysis of the governing equations has been added and the effects of the thermal asymmetry and heat generation/absorption are the novel and distinctive outcomes of this study which

have been considered.

2. PROBLEM DESCRIPTION

Consider a steady fully developed laminar flow of alumina/water nanofluid inside a vertical microchannel in the presence of heat source/sink which is oriented along the gravitational direction. The physical model is illustrated in Fig. 1, where the Cartesian coordinates x and y are aligned vertically and normal to the walls, respectively. The walls are heated uniformly by external means at a rate of q''_{wr} and q''_{wl} for the right and left walls, respectively. The ratio of the heat fluxes is $\varepsilon = q''_{wl} / q''_{wr}$, which characterizes the degree of the thermal asymmetry.

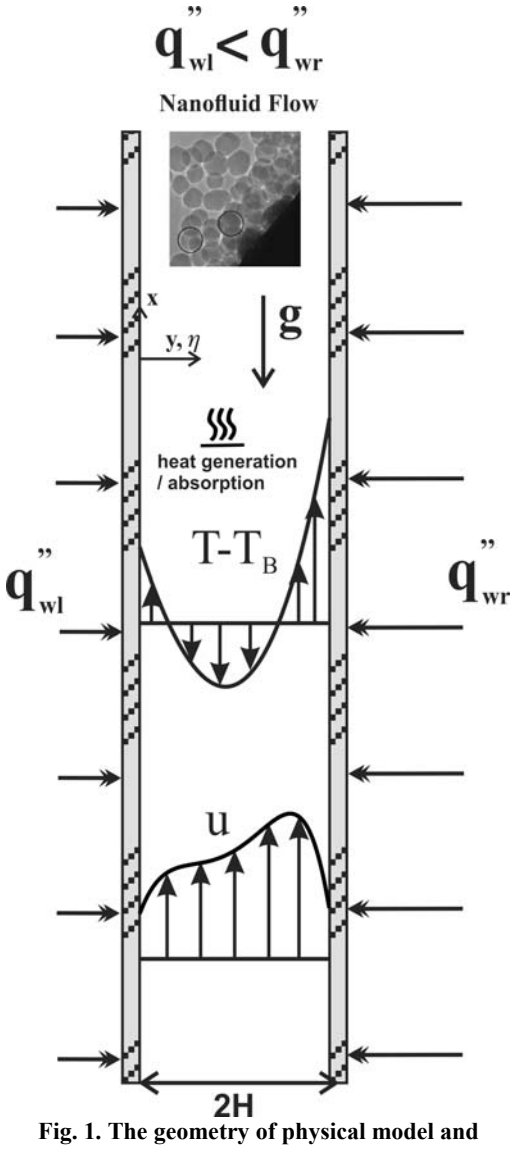

Fig. 1. The geometry of physical model and coordinate system.

From the numerical solutions provided by Koo and Kleinstreuer (2005) for the most standard nanofluid flows inside a channel of around 50μm, the viscous dissipation is negligible. The flow has been assumed to be laminar, incompressible, and hydrodynamically and thermal fully developed. In addition, there are no chemical reaction and external forces in the flow and local thermal equilibrium has been assumed between nanoparticles and the base fluid. Consequently, the basic incompressible conservation equations of the mass, momentum, thermal energy, and nanoparticle fraction can be expressed in the following manner (Malvandi *et al*. (2014), Yang *et al*. (2013)):

Momentum equation

$$\frac{d}{dy}\left(\mu\frac{du}{dy}\right)-\frac{dP}{dx} + \begin{bmatrix}(1-\phi_{wr})\rho_{f0}\beta(T-T_B)\\ -(\rho_f-\rho_{f0})(\phi-\phi_{wr})\end{bmatrix} g = 0 \tag{1}$$

Energy equation

$$\rho c_p u\frac{\partial T}{\partial x}=\frac{\partial}{\partial y}\left(k\frac{\partial T}{\partial y}\right)+Q_0(T-T_B) + \rho_p c_p\left(D_B\frac{\partial\phi}{\partial y}+\frac{D_T}{T}\frac{\partial T}{\partial y}\right)\frac{\partial T}{\partial y} \tag{2}$$

Nanoparticle flux equation

$$\frac{\partial}{\partial y}\left(D_B\frac{\partial\phi}{\partial y}+\frac{D_T}{T}\frac{\partial T}{\partial y}\right)=0 \tag{3}$$

where u, T and P represent the axial velocity, local temperature and pressure, respectively. Moreover, the Brownian diffusion coefficient D_B and thermophoretic diffusion coefficient D_T are defined

$$D_B=\frac{k_{BO}T}{3\pi\mu_{bf}d_p} \tag{4}$$

and

$$D_T=0.26\frac{k_{bf}}{2k_{bf}+k_p}\frac{\mu_{bf}}{\rho_{bf}}\phi \tag{5}$$

respectively, where k_{BO} is the Boltzmann constant and d_p is the nanoparticle diameter. Further, ρ, μ, k, c are the density, dynamic viscosity, thermal conductivity, and specific heat capacity of Al_2O_3-water nanofluid respectively, depending on the nanoparticle volume fraction as follows

$$\begin{aligned}&\mu=\mu_{bf}(1+39.11\phi+533.9\phi^2),\\ &\rho=\phi\rho_p+(1-\phi)\rho_{bf},\\ &c_p=\left(\phi\rho_p c_{p_p}+(1-\phi)\rho_{bf}c_{p_{bf}}\right)/\rho,\\ &k=k_{bf}(1+7.47\phi),\\ &\beta=\frac{\phi\rho_p\beta_p+(1-\phi)\rho_{bf}\beta_{bf}}{\rho}\end{aligned} \tag{6}$$

and the thermophysical properties of water/alumina nanoparticle and base fluid (water) are also provided as follows Pak and Cho (1998) :

$$\begin{aligned} &c_{p_{bf}} = 4182 \text{ J/(KgK)}, \rho_{bf} = 998.2\ Kg/m^3 \\ &k_{bf} = 0.597 \text{ W/(mK)}, k_p = 36 \text{ W/(m K)} \\ &c_{p_p} = 773 \text{ J/(Kg K)}, \rho_p = 3880\ Kg/m^3 \\ &\mu_{bf} = 9.93\times10^{-4} \text{ Kg/(ms)} \end{aligned} \tag{7}$$

where *bf* stands for the base fluid and *p* for particle. Also, the boundary conditions can be expressed as

$$\begin{aligned} &y = 0 : u = N\frac{\mu_{wl}}{\rho_{wl}}\frac{du}{dy}, -k\frac{\partial T}{\partial y} = q''_{wl}, \\ &D_B\frac{\partial \phi}{\partial y} + \frac{D_T}{T}\frac{\partial T}{\partial y} = 0. \\ &y = 2H : u = -N\frac{\mu_{wr}}{\rho_{wr}}\frac{du}{dy}, k\frac{\partial T}{\partial y} = q''_{wr}, \\ &D_B\frac{\partial \phi}{\partial y} + \frac{D_T}{T}\frac{\partial T}{\partial y} = 0. \end{aligned} \tag{8}$$

where N represents slip velocity factor. In Eq. (8), $D_B(\partial\phi/\partial y) + D_T/T(\partial T/\partial y) = 0$ is obtained due to impermeable boundary conditions at the walls (Buongiorno (2006), Yang *et al*. (2013)) which means that Brownian diffusion and thermophoresis should be cancel out each other. Eqs. (1)-(3) can be simplified with the scale analysis. Let us consider our physical conditions, which are typically occurring in the flow of alumina/water nanofluids inside microchannels. Table 1 shows the device and material properties of typical water-based nanofluid with alumina nanoparticles, from which one can calculate the coefficients of the governing equations.

Table 1 Device and material properties of alumina/water nanofluid

u_{ref} (m/s)	ϕ_{ref}	μ_{ref} kg/ m.s	$L_{ref} = H$ m	β $1/K$
0.01	0.02	0.00198	7.5 .10^{-5}	2.10^{-4}
$(T - T_B)_{ref}$ K	ρ_p kg/m^3	ρ_f kg/m^3	Q W/ m^{3}K	g m/s^2
50	3880	998.2	2.10^7	10

Considering Eq. (1), the scale analysis can be written as follows

$$\frac{\Delta p}{L_{ref}} \approx \begin{pmatrix} \underbrace{\frac{\mu\Delta U}{L_{ref}^2}}_{3.52\times10^3}, \\ \underbrace{(1-\phi)\rho_{bf} g\beta\Delta T}_{101}, \\ \underbrace{(\rho_p - \rho_{f0})g\Delta\phi}_{2.8\times10^4} \end{pmatrix} \tag{9}$$

From Eq. (9) it can be concluded that the buoyancy effects due to the temperature gradient (second RHS term) are negligible with respect to the buoyancy effects due to nanoparticle distribution (third RHS term) and also the shear stress terms (first RHS term). Thus, this term can be neglected from Eq. (1). On the other hand, the scale analysis for Eq. (2) can be expressed as

$$\begin{aligned} &LHS: \underbrace{\begin{pmatrix} \phi_B\rho_p c_{p_p} + \\ (1-\phi_B)\rho_{bf} c_{p_{bf}} \end{pmatrix}\frac{U_{ref}\Delta T}{\Delta x}}_{2.0285\times10^8} \\ &\text{RHS}: \underbrace{k_{bf}(1+7.47\phi_B)\frac{\Delta T}{L_{ref}^2}}_{2.086\times10^{10}}, \underbrace{Q\Delta T}_{10^9}, \\ &\underbrace{\rho_p c_{p_p}}_{3\times10^6}\begin{pmatrix} \underbrace{\frac{D_\phi\Delta\phi}{L_{ref}}}_{1.97\times10^{-7}} + \\ \underbrace{\frac{D_T\Delta T}{T_{ref}L_{ref}}}_{5.54\times10^{-7}} \end{pmatrix}\underbrace{\frac{\Delta T}{L_{ref}}}_{6.67\times10^5} \end{aligned} \tag{10}$$

Above scale analysis indicated that the LHS term is in the same order of magnitude with the first and second terms of RHS term and these are about 10^5 times more than the third term of it. In fact, heat transfer associated with nanoparticle diffusion (third RHS term) can be neglected in comparison with the other terms. Hence, the governing equations (Eqs. (1)-(3)) can be given as:

$$\begin{aligned} &\frac{d}{dy}\left(\mu\frac{du}{dy}\right) - \frac{dp}{dx} - \\ &\left(\rho_p - \rho_{f0}\right)\left(\phi - \phi_{wr}\right)g = 0 \end{aligned} \tag{11}$$

$$\begin{aligned} &\rho c_p u\frac{\partial T}{\partial x} + Q_0(T - T_B) \\ &-\frac{\partial}{\partial y}\left(k\frac{\partial T}{\partial y}\right) = 0 \end{aligned} \tag{12}$$

$$\frac{\partial}{\partial y}\left(D_B\frac{\partial\phi}{\partial y} + \frac{D_T}{T}\frac{\partial T}{\partial y}\right) = 0 \tag{13}$$

Equation (12) indicated that the energy equation for nanofluid is in the same form of regular fluid. As a result, the heat transfer in nanofluids only affected via the rheological and thermophysical properties which depend on nanoparticle distribution. After solving the equations, the average value of parameters required should be calculated over the cross-section by

$$\overline{\varphi} \equiv \frac{1}{A}\int_A \varphi dA = \frac{1}{2H}\int_0^{2H}\varphi dy \tag{14}$$

and the bulk mean temperature is defined as

$$T_B \equiv \frac{\overline{\rho c_p u T}}{\overline{\rho c_p u}} \tag{15}$$

Due to the constant diffusion mass flux of nanofluid (Eq. (13)) and the impermeable wall condition, everywhere in the annulus, the Brownian diffusion flux and thermophoretic diffusion flux is canceled out ($D_B\frac{\partial\phi}{\partial y} = -\frac{D_T}{T}\frac{\partial T}{\partial y}$). By averaging Eq. (2) from

$y = 0$ to $2H$ and according to the thermally fully developed condition for the uniform wall heat flux ($dT/dx = dT_B/dx$) and introducing the following non-dimensional parametrs:

$$\eta = \frac{y}{2H},\ u^* = \frac{u}{\frac{H^2}{\mu_{wr}}\left(-\frac{dp}{dx}\right)},$$

$$T^* = \frac{T - T_B}{q''_{wr} H / k_{wr}},\ \gamma = \frac{q''_{wr} H}{k_{wr} T_B}$$

$$N_{BT} = \frac{D_{B_B} k_{wr} T_B \phi_B}{D_{T_B} H q''_{wr}},\ \sigma = \frac{Q_0 H^2}{k_{bf}},$$

$$Nr = \frac{g(\rho_f - \rho_{f0})}{\left(-\frac{dp}{dx}\right)},\ \varepsilon = \frac{q''_{wl}}{q''_{wr}}$$

Eqs. (11)-(13) can be reduced as

$$\frac{d^2 u^*}{d\eta^2} = -\frac{1}{\mu}\frac{d\mu}{d\phi}\frac{d\phi}{d\eta}\frac{du^*}{d\eta} - \frac{4\mu_{wr}}{\mu}\left(1 - Nr\left(\phi - \phi_{wr}\right)\right) \quad (16)$$

$$\frac{d^2 T^*}{d\eta^2} = \left[\begin{array}{l} \frac{k_{wr}}{k}\left(\frac{2(1+\varepsilon) + \frac{4\sigma}{1+7.47\phi_{wr}}\overline{T^*}}{\overline{\rho c u^*}}\right)\overline{\rho c u^*} \\ -\frac{4\sigma}{1+7.47\phi_{wr}}T^* - \frac{1}{k_{wr}}\frac{dk}{d\phi}\frac{d\phi}{d\eta}\frac{dT^*}{d\eta} \end{array}\right] \quad (17)$$

$$\frac{\partial\phi}{\partial\eta} = -\frac{\phi}{N_{BT}(1+\gamma T^*)^2}\frac{\partial T^*}{\partial\eta} \quad (18)$$

with the boundary conditions

$$\eta = 0:$$

$$u^* = \lambda\frac{1 + 39.11\phi_{wl} + 533.9\phi_{wl}^2}{\phi_{wl}\,\rho_p/\rho_{bf} + (1-\phi_{wl})}\frac{du^*}{d\eta},$$

$$\frac{\partial T^*}{\partial\eta} = -2\varepsilon\frac{k_{wr}}{k_{wl}}.$$

$$\eta = 1:$$

$$u^* = -\lambda\frac{1 + 39.11\phi_{wr} + 533.9\phi_{wr}^2}{\phi_{wr}\,\rho_p/\rho_{bf} + (1-\phi_{wr})}\frac{du^*}{d\eta},$$

$$\text{a}\ \ \frac{\partial T^*}{\partial\eta} = 2,\quad \phi = \phi_{wr}. \quad (19)$$

where the slip parameter λ, the bulk mean dimensionless temperature T_B^* and the bulk mean nanoparticle volume fraction ϕ_B can be obtained

$$\phi_B = \frac{\overline{u^*\phi}}{\overline{u^*}},\ \lambda = N\frac{\mu_{bf}}{2H\rho_{bf}} \quad (20)$$

The Nusselt number at the left wall is defined as.

$$Nu_{wl} = \frac{h_{wl}D_h}{k_{wl}} = \frac{4\varepsilon}{T_{wl}^*}\frac{k_{wr}}{k_{wl}} \quad (21)$$

and, at the right wall

$$Nu_{wr} = \frac{h_{wr}D_h}{k_{wr}} = \frac{4}{T_{wr}^*} \quad (22)$$

The Nusselt number based on the thermal conductivity of base fluid can be defined as the non-dimensional heat transfer coefficient by

$$\frac{hD_h}{k_{bf}} = Nu\frac{k}{k_{bf}} = Nu\left(1 + 7.47\phi\right) \quad (23)$$

So, the total heat transfer coefficient enhancement and pressure drop may be evaluated as

$$\frac{h_{tot}}{h_{tot\ (bf)}} = \frac{Nu_{wl} + Nu_{wr}}{\left(Nu_{wl} + Nu_{wr}\right)_{bf}}\left(1 + 7.47\phi\right) \quad (22)$$

$$N_{dp} = \frac{-\frac{dp}{dx}}{\mu_{bf}\frac{u_B}{(4H)^2}} = \frac{16\rho_B}{\overline{\rho u^*}\left(\mu_{bf}/\mu_{wr}\right)} \quad (23)$$

3. NUMERICAL MODEL AND ACCURACY

The Eqs. (17)-(19) are solved in conjuction with the boundary conditions of Eq. (20) by means of the Runge-Kutta-Fehlberg scheme. A Fortran code has been used to find the numerical solution of the present boundary value problem (BVP), the accuracy of which is shown elsewhere Malvandi *et al*. (2013),Malvandi *et al*. (2014) . Convergence criterion is considered to be 10^{-6} for relative errors of the velocity, temperature, and nanoparticle volume fraction. The numerical procedure involves a reciprocal algorithm in which ϕ_w, $\overline{\rho c_p u^*}$, and $\overline{T^*}$ are used to calculate the value of ϕ_B, $\overline{\rho c_p u^*}$, and $\overline{T^*}$. The process is repeated until a prescribed value of ϕ_B reached, and the relative error between the assumed values of $\overline{\rho c_p u^*}$ and $\overline{T^*}$ with the calculated ones after solving Eqs. (17)-(19) is lower than 10^{-6}. In view of helping others to regenerate their own results and provide possible future references, the numerical algorithm is shown graphically in Fig. 2.

To check the accuracy of the numerical code, the results obtained for a horizontal parallel-plate channel with $Nr = \lambda = \sigma = 0$, and $\varepsilon = 1$ are compared to the reported results of Yang *et al*. (2013) in Table 2. Obviously, the results are in a desirable agreement. It must be mentioned that all the numeric results obtained here are carried out using the integration step $d\eta = 10^{-6}$.

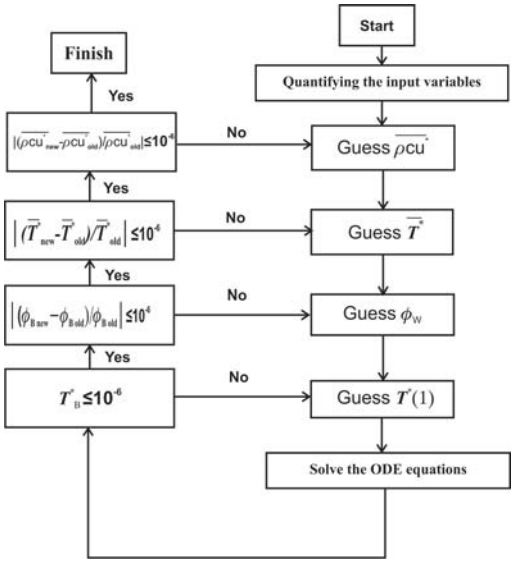

Fig. 2. Algorithm of the numerical method.

Table 2 Comparison of numerical results with the ones reported by Yang *et al.* (2013) when $Nr=\sigma=\lambda=0, \varepsilon=1$**.**

ϕ_B	N_{BT}	Yang *et al.* (2013)		Present work	
		Nu	N_{dp}	Nu	N_{dp}
0.02	0.2	7.9486	30.975	7.95	30.776
	0.5	8.1393	37.925	8.141	37.47
	1	8.1890	42.098	8.192	41.742
	2	8.2139	44.732	8.210	44.558
	5	8.2346	46.488	8.225	46.532
0.06	0.2	7.534	18.854	7.540	18.627
	0.5	7.9361	29.667	7.923	29.498
	1	8.0771	36.784	7.961	36.590
	2	8.1476	41.589	8.016	41.521

4. RESULTS AND DISCUSSION

Migration of nanoparticles, the viscosity and thermal conductivity distributions are determined by the mutual effects of the Brownian diffusion and the thermophoresis. Here, these effects are considered by means of N_{BT}, which is the ratio of Brownian diffusion to the thermoporesis. With $d_p \cong 20nm$ and $\phi_B \cong 0.1$, the ratio of Brownian motion to thermophoretic forces N_{BT}~1/dp can be changed over a wide range of 0.2 to 10 for alumina/water nanofluid. In addition, $\gamma \cong \frac{T_w - T_B}{T_w}$ may change from 0 to 0.2, however, its effects on the solution is insignificant (see Refs. Yang *et al*. (2013),Yang *et al*. (2013)); so the results has been carried for $\gamma \cong 0.1$.

Figs. **3-6** show the effects of $\varepsilon, \sigma, \lambda,$ and Nr, respectively, on the velocity (u/u_B), temperature (T^*), and nanoparticle volume fraction (ϕ/ϕ_B) profiles. The left wall is placed in $\eta=0$, whereas $\eta=1$ corresponds to the right wall.

Regarding Fig. **3**, for $\varepsilon<1$ the nanoparticle accumulation region is formed near the left wall, having a lower heat flux. Increasing ε shifts the peak of the nanoparticle volume fraction toward the middle of the channel such that for $\varepsilon=1$ (thermal symmetry at the walls), the nanoparticle distribution becomes symmetric and nanoparticle accumulated region formed in the middle of the microchannel. Further, an increase in ε leads the peak of the nanoparticle concentration to move toward the right wall. This is due to the fact that the thermophoresis, which is related to the temperature gradient, is the mechanism of the nanoparticle migration. Any change in ε leads the temperature gradient at the walls to change, so changes the thermophoresis. For $\varepsilon<1$, the temperature gradient at the right wall is more than that at the left wall; so the nanoparticle migration from the right wall is greater, leading the nanoparticle accumulated region moves toward the left wall. This phenomena continues until $\varepsilon=0$, in which there is no temperature gradient at the left wall; so a nanoparticle accumulation region formed on the left wall. The effects of ε on nanoparticles concentration have considerable influence on the velocity and temperature profiles. Obviously, the velocity and temperature profiles are symmetric for $\varepsilon=1$, in which the nanoaprticle volume fraction is symmetric. For $\varepsilon<1$ the regular symmetry in the velocity profile disappears and the peak of the velocity profile shifts toward the right wall (the lower viscosity region), as ε decreases. However, the dip point of the temperature profile increases and moves toward the left wall in which the nanoparticles accumulated (the higher thermal conductivity region). In fact, the velocity profile has a tendency to shift toward the nanoparticle depleted region, however, for the temperature profile it is the opposite.

The effects of σ is shown in Fig. 4. When there is a heat absorption ($\sigma<0$), more energy will be absorbed by the fluid; so the dip of the temperature profile decreases. In fact, the temperature profile becomes to be more uniform for the negative values of σ. This leads to an increase and a decrease in the temperature gradients at the left and right walls, respectively. Increasing the temperature gradient at the left wall enhances the nanoparticle migration there, whereas a drop in the temperature gradient at the right wall reduces the nanoparticle migration. Accordingly, the peak of the nanoparticle concentration decreases and nanoparticle distribution becomes more uniform; so, the velocity profile moves back toward the central region. In contrast, heat generation ($\sigma>0$) increases the temperature gradients at the right wall and increases the nanoparticle migration there, whereas for the left wall it is the opposite. This is the reason that in the presence of heat generation, the velocity profiles moves toward the right wall.

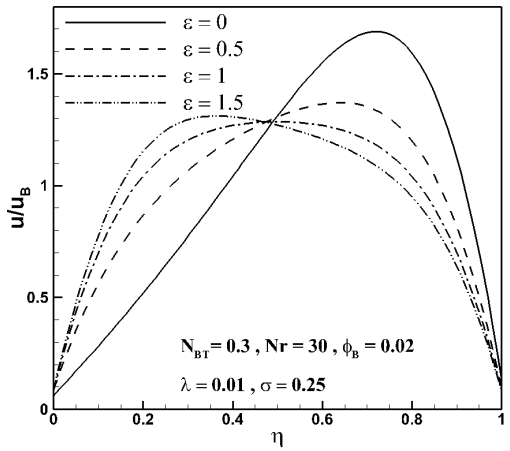

(a)

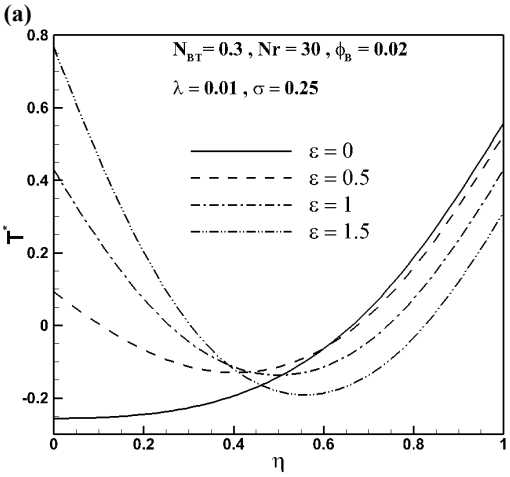

(b)

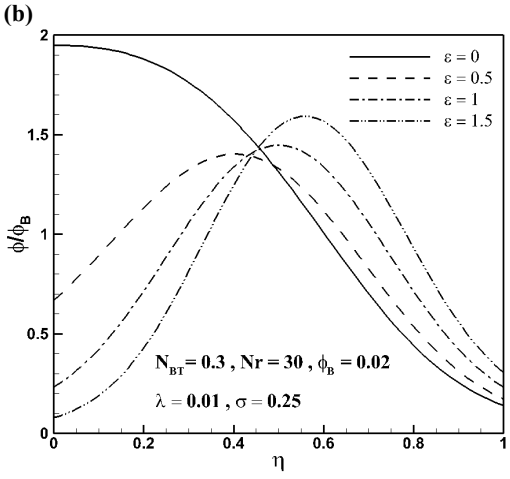

(c)

Fig. 3. The effects of ε on (a) velocity (u/u_B), (b) temperature (T^*), and (c) nanoparticle distribution (ϕ/ϕ_B) profiles when $Nr = 30$, $N_{BT} = 0.3$, $\sigma = 0.25$, $\phi_B = 0.02$ and $\lambda = 0.01$.

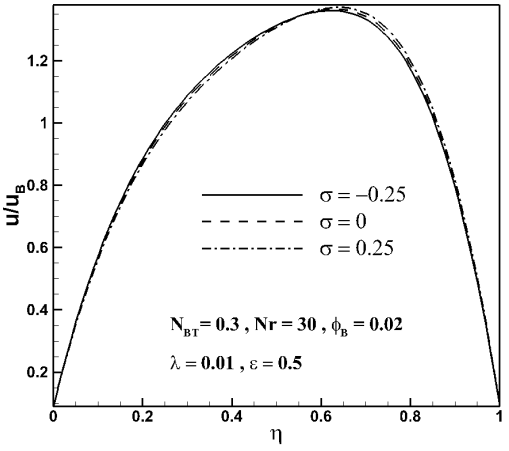

(a)

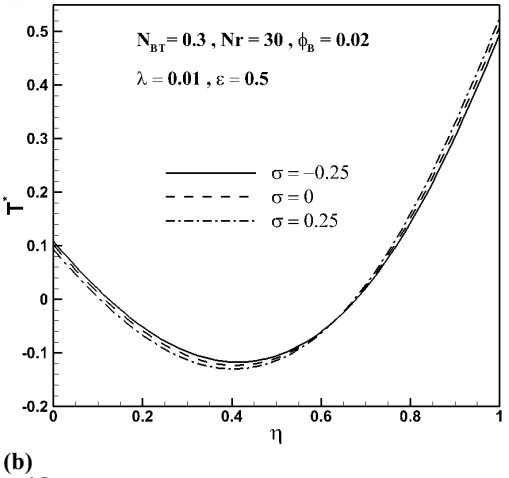

(b)

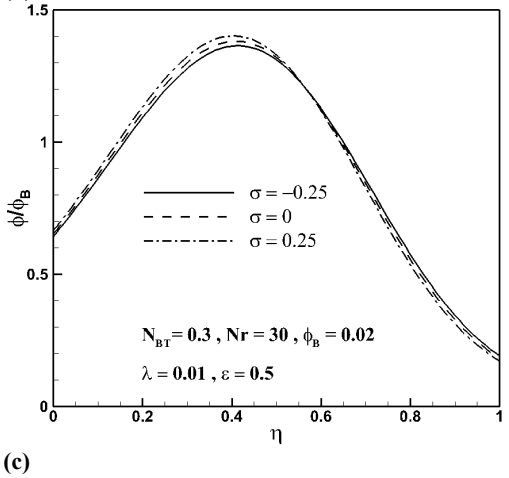

(c)

Fig. 4. The effects of σ on (a) velocity (u/u_B), (b) temperature (T^*), and (c) nanoparticle distribution (ϕ/ϕ_B) profiles when $Nr = 30$, $N_{BT} = 0.3$, $\varepsilon = 0.5$, $\phi_B = 0.02$ and $\lambda = 0.01$.

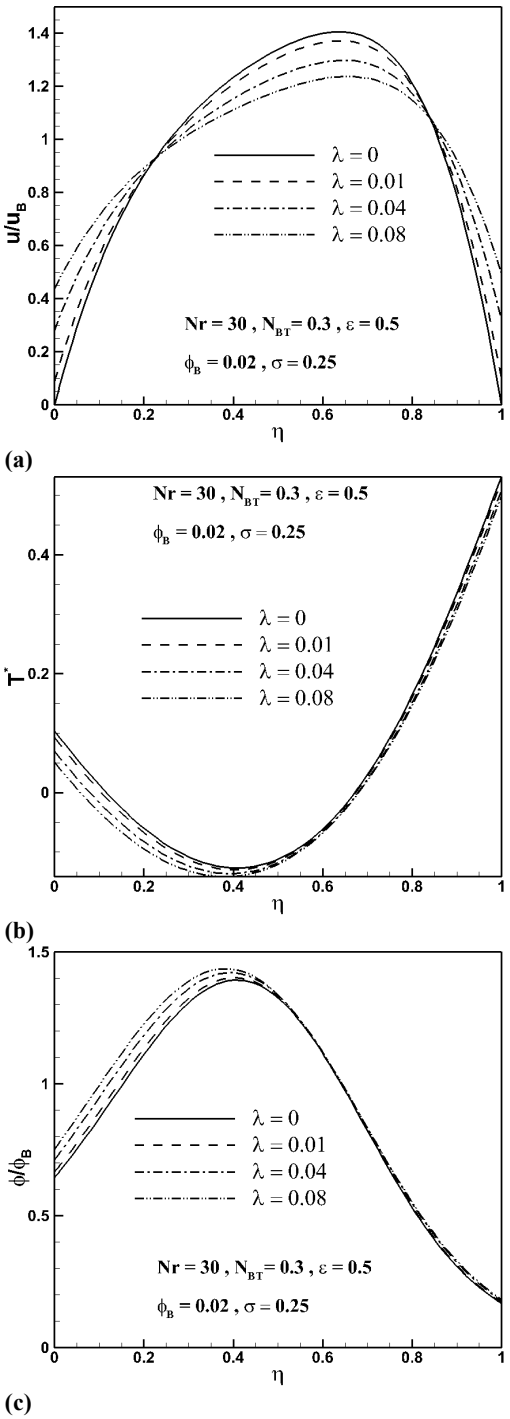

Fig. 5. The effects of λ on (a) velocity (u/u_B), (b) temperature (T^*), and (c) nanoparticle distribution (ϕ/ϕ_B) profiles when $Nr = 30$, $N_{BT} = 0.3$, $\varepsilon = 0.5$, $\phi_B = 0.02$ and $\sigma = 0.25$.

The effects of the slip parameter is shown in Fig. **5**. It is obvious that the slip parameter λ signifies the amount of slip velocity at the surface. Increasing λ leads to a rise in the slip velocity closer to the walls and because of the constant mass flow rate in the channel, the velocity in the core region reduces. In other words, the momentum in the core region shifts toward the walls and leads to a more uniform velocity profile, as λ increases. The momentum enrichments near the walls increase the heat removal ability of the flow and reduces the walls' temperature and its gradient. As a result, the nanoparticle migration from the heated walls reduces.

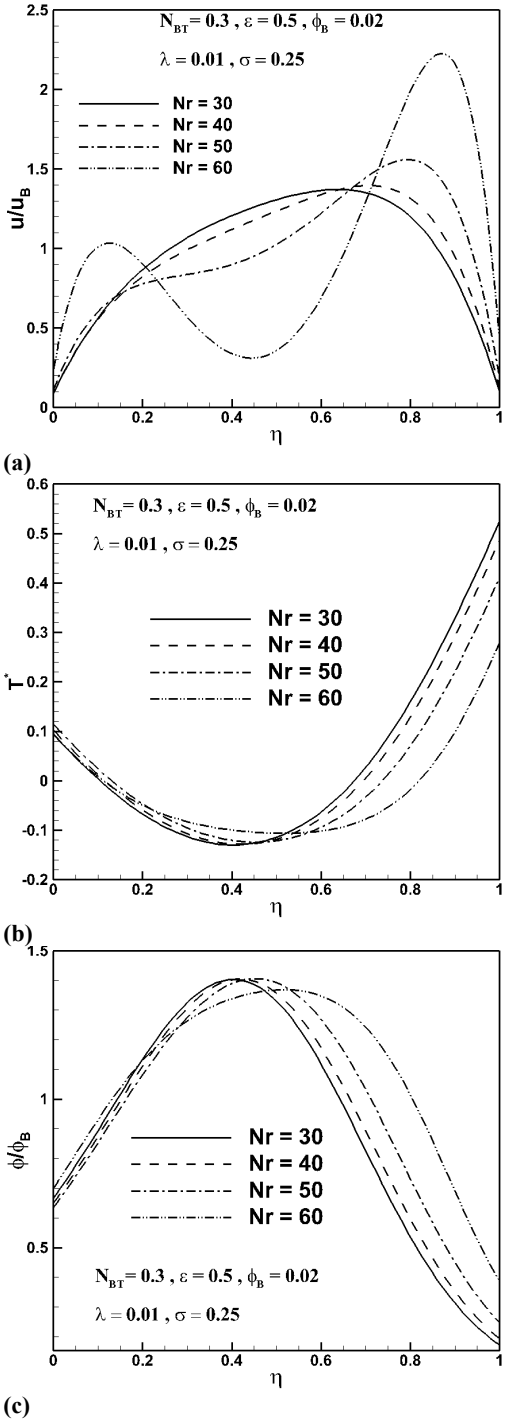

Fig. 6. The effects of *Nr* on (a) velocity (u/u_B), (b) temperature (T*), and (c) nanoparticle distribution (ϕ/ϕ_B) profiles when $\lambda = 0.01$, $N_{BT} = 0.3$, $\varepsilon = 0.5$, $\phi_B = 0.02$ and $\sigma = 0.25$.

Finally, an examination of Fig. **6** reveals a gradual

increase of the velocities of the fluid closed to the walls (the low viscosity region), followed by a decrease in the core region, as *Nr* increases. In fact, all of the incoming fluid is forced to move slowly close to the walls. Obviously, the momentum enrichments near the right wall (which has the lowest viscosity) are greater and reduce the temperature significantly. In addition, increasing *Nr* shifts the peak of the nanoparticle volume fraction toward the right wall and reduces the intensity of the nanoparticle depletion there.

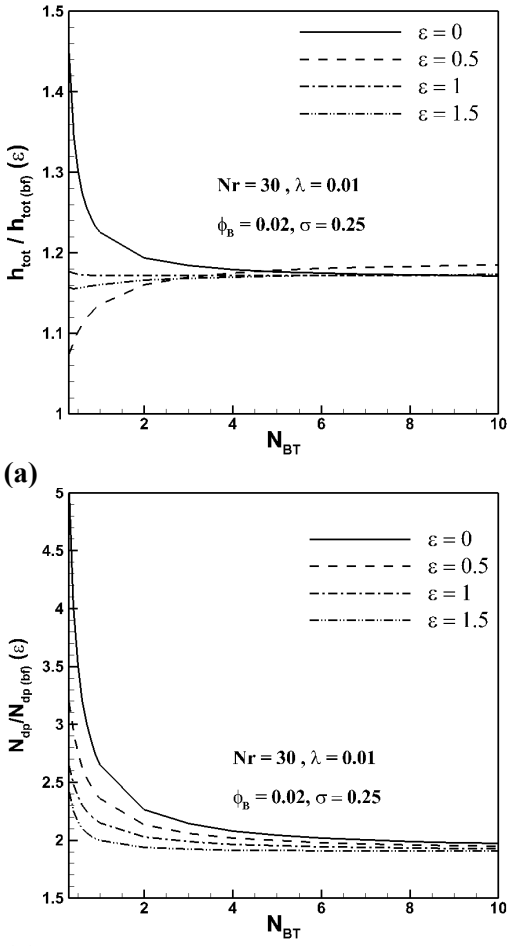

Fig. 7. The effects of ε on the heat transfer coefficient ratio (a), and the pressure drop ratio (b) when $\lambda = 0.01$, $Nr = 30$, $\phi_B = 0.02$ and $\sigma = 0.25$.

Figs. **7** to **10** show the effects of the parameters ε, σ, λ, and *Nr* respectively, on (a) the heat transfer ratio, and (b) the pressure drop ratio. Regarding the figures, the pressure drop ratio has a decreasing trend with increasing N_{BT}. Routinely, N_{BT} is higher for smaller nanoparticles ($N_{BT} \sim D_B \sim 1/d_p$); so using smaller nanoparticle reduces the increment of the pressure drop.

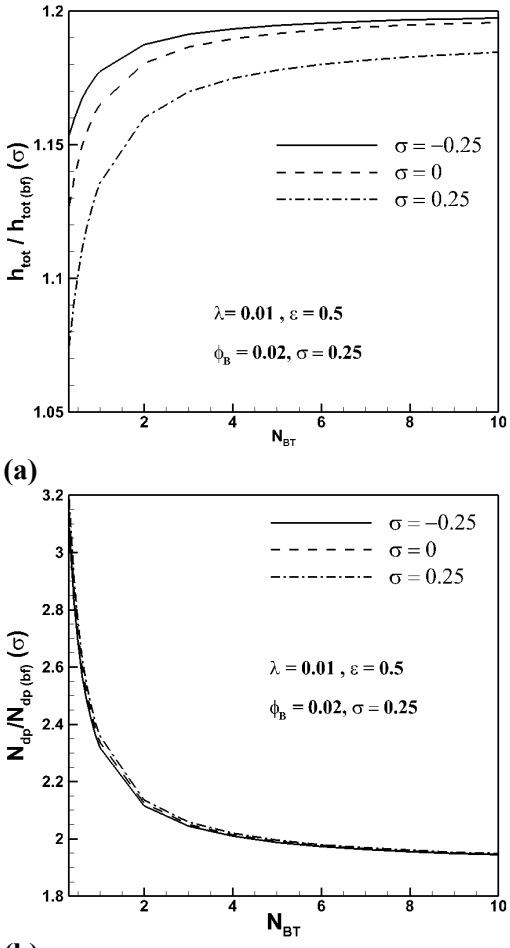

Fig. 8. The effects of σ on the heat transfer coefficient ratio (a), and the pressure drop ratio (b) when $\varepsilon = 0.5$, $Nr = 30$, $\phi_B = 0.02$ and $\lambda = 0.01$.

From Fig. **7**, it is obvious that the heat flux ratio ε has significant effects on the heat transfer enhancement. Also, the variations of heat transfer enhancement with N_{BT} is considerably affected by ε. It can be seen that for the symmetric thermal boundary condition ε=1, heat transfer enhances about 20% from all the values of N_{BT} which varies from 0.2 to 10. Employing asymmetric heat flux at the surfaces, reduces the heat transfer enhancement for the lower values of N_{BT}. However, for the higher values of N_{BT}, the heat transfer rate slighty increases. This is because with decreasing ε, the momentum enriches at the right wall and increases the advantage of the nanoparticle inclusion there (see Fig. 3a), however, the impoverishment of the local velocities at the left wall decreases the heat trasnfer rate. This phenomena is considerable for the lower values of N_{BT} where the nanoparticle migration is significant.

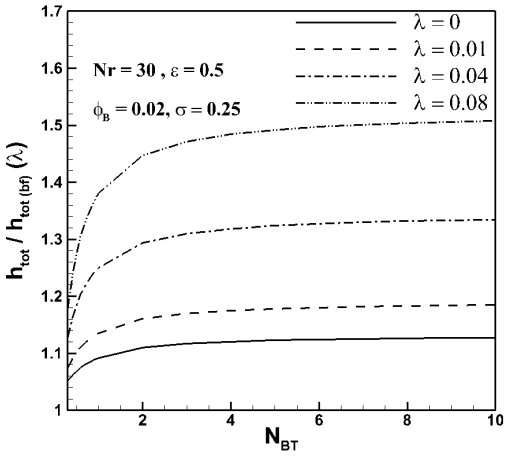

(a)

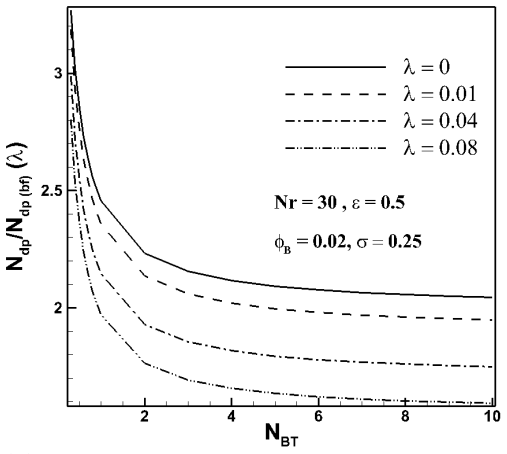

(b)

Fig. 9. The effects of λ on the heat transfer coefficient ratio (a), and the pressure drop ratio (b) when $\varepsilon = 0.5$, $Nr = 30$, $\phi_B = 0.02$ and $\sigma = 0.25$.

In addition, increasing the thermal conductivity at the left wall (nanoparticle accumulated region) enhances the heat transfer rate there, whereas for the right wall it is the opposite. In each wall thus there are two mechanisms that act against each other and the net result of these phenomena determines the overall heat transfer ratio. The reduction in the heat transfer enhancement for $\varepsilon < 1$ at lower values of N_{BT}, indicates that the decreasing rate of the heat transfer rate at the left wall is dominant, whereas for the larger values of N_{BT} it is the opposite. But, for $\varepsilon = 0$, where the left wall is adiabatic, there is no reduction in the heat transfer rate at the left wall; so, the heat transfer enhanement follows the enhancement at the right wall. In this case, for the lower values of N_{BT}, the momentum enrichment at the right wall leads to maximum about 45% enhancement in heat transfer rate; but for the higher values of N_{BT}, the reduction in the thermal conductivity leads to a lower enhancement of heat transfer rate with respect of the other cases. Thus, it can be concluded that one sided heating (one of the walls kept adiabatic) leading to the best heat transfer enhancement for larger nanoparticles (the lower values of N_{BT}). However, for the smaller nanoparticles, where there is no significant migration of nanoparticle, one sided heating has not considerable influence on the heat transfer and the pressure drop ratios.

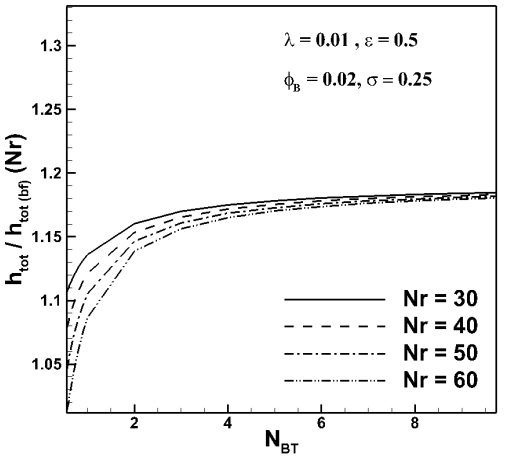

(a)

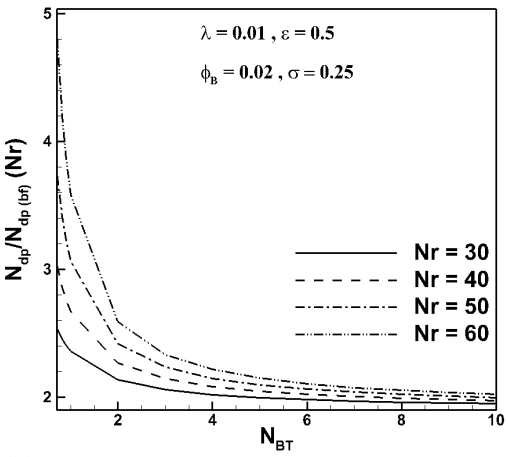

(b)

Fig. 10. The effects of Nr on the heat transfer coefficient ratio (a), and the pressure drop ratio (b) when $\lambda = 0.01$, $\varepsilon = 0.5$, $\phi_B = 0.02$ and $\sigma = 0.25$.

Fig. **8** shows that the heat transfer rate increases in the presence of heat absorption ($\sigma < 0$), while it decreases in the case of heat generation. In addition, there is no significant change in the pressure drop ratio; so, the performance of the system is increased in the presence of heat absorption. Regarding Fig. **9**, the heat transfer ratio is increased with increasing the slip parameter λ, however, an inverse trend can be observed for the pressure drop ratio. Decreasing the pressure drop (N_{dp}) is a useful attribute, particularly in microchannels where the head loss extremely pronounced, since it allows a significant reduction in the pumping power required to drive the nanofluid flow. Accordingly, the slip velocity is a positive phenomena in the current heat transfer system since it allows the heat transfer enhancement followed by a reduction in the pressure drop.

Finally, Fig. **10** indicates that the mixed convection due to the non-uniform nanoparticle distribution has a negative effect on the performance of the system; because increasing Nr leads to a rise in the pressure drop ratio and reduces the heat transfer enhancement. This effect significantly depends on the nanoparticle size (N_{BT}); using smaller nanoaprticles prevents the reduction of the performance of the system which originates from the mixed convection effects.

5. CONCLUSION

Fully developed mixed convective heat transfer of alumina/water nanofluid inside a vertical microchannel in the presence of heat source/sink with asymmetric wall heating has been investigated theoretically. Walls are subjected to different heat fluxes; q''_{wl} for the left wall and q''_{wr} for the right wall. The modified two-component heterogeneous model is employed for the nanofluid in the hypothesis that the Brownian motion and the thermophoresis are the only significant bases of nanoparticle migration. The basic partial differential equations including continuity, momentum, energy, and nanoparticle volume fraction equations have been reduced to two-point ordinary boundary value differential equations before they are solved numerically. The major findings of this paper can be expressed as:

- Because of the thermophoresis, the nanoparticles migrate from the heated walls (making a depleted region) and accumulated at central regions of the channel, more likely to accumulate near the wall with the lower heat flux. As a result, an in-homogeneous distribution of nanoparticles developed which leads to a non-uniform distribution of the viscosity and thermal conductivity of nanofluids.

- For $\varepsilon = \frac{q''_{lw}}{q''_{rw}} < 1$, a regular symmetry in the velocity profile disappears and the peak of the velocity profiles shifts toward the right wall, where the nanoparticle depleted region is located (lower viscosity). However, the dip point of the temperature profile moves toward the left wall in which the nanoparticles accumulated (higher thermal conductivity). In fact, the velocity profile has a tendency to shift toward the nanoparticle depleted region, however, for the temperature profile it is the opposite.

- Asymmetric heating at the walls, prevents the enrichment of the velocities at the walls, reducing the heat transfer enhancement with respect to the symmetric heating. However, one sided heating (one wall is kept adiabatic) intensifies the heat transfer enhancement.

- Increasing the mixed convective parameter *Nr* reduces the heat transfer rate, which is more pronounced for larger nanoparticles.

- The heat transfer rate enhances in the presence of heat absorption, while it decreases in the case of heat generation. In addition, there is no significant change in the pressure drop ratio; so, the performance of the system is increased in the presence of heat absorption.

- The slip parameter λ has an important role in the heat transfer enhancement of the microchannels. The heat transfer rate has an increasing trend with λ and due to the smoother velocity gradients at the channel's walls, the pressure drop N_{dp} has a decreasing trend. In essence, slip velocity at the walls enhances the performance of heat transfer systems.

REFERENCES

Ashorynejad, H. R., A. A. Mohamad and M. Sheikholeslami (2013). Magnetic field effects on natural convection flow of a nanofluid in a horizontal cylindrical annulus using Lattice Boltzmann method. *International Journal of Thermal Sciences* 64(0), 240-250.

Buongiorno, J. (2006). Convective Transport in Nanofluids. *Journal of Heat Transfer* 128(3), 240-250.

Cheng, C. H., H. S. Kou and W. H. Huang (1990). Flow reversal and heat transfer of fully developed mixed convection in vertical channels. *Journal of Thermophysics and Heat Transfer* 4(3), 375-383.

Choi, S. U. S. (1995). Enhancing thermal conductivity of fluids with nanoparticles. *in Developments and Applications of Non-Newtonian Flows, D. A. Siginer and H. P. Wang, Eds., ASME* 66, 99-105.

Ganji, D. D. and A. Malvandi (2014). Natural convection of nanofluids inside a vertical enclosure in the presence of a uniform magnetic field. *Powder Technology* 263(0), 50-57.

Hedayati, F., A. Malvandi, M. H. Kaffash and D. D. Ganji (2015). Fully developed forced convection of alumina/water nanofluid inside microchannels with asymmetric heating. *Powder Technology* 269, 520-531.

Hedayati, F. and G. Domairry (2015). Effects of nanoparticle migration and asymmetric heating on mixed convection of TiO2–H2O nanofluid inside a vertical microchannel. *Powder Technology* 272, 250-259.

Hwang, K. S., S. P. Jang and S. U. S. Choi (2009). Flow and convective heat transfer characteristics of water-based Al2O3 nanofluids in fully developed laminar flow regime. *International Journal of Heat and Mass Transfer* 52(1–2), 193-199.

Koo, J. and C. Kleinstreuer (2005). Laminar nanofluid flow in microheat-sinks. *International Journal of Heat and Mass Transfer* 48(13), 2652-2661.

Kuznetsov, A. V. and D. A. Nield (2010). Natural convective boundary-layer flow of a nanofluid past a vertical plate. *International Journal of Thermal Sciences* 49(2), 243-247.

Mahmoodi, M. and S. M. Hashemi (2012). Numerical study of natural convection of a nanofluid in C-shaped enclosures. *International Journal of Thermal Sciences* 55(0), 76-89.

Malvandi, A. and D. D. Ganji (2014). Brownian motion and thermophoresis effects on slip flow of alumina/water nanofluid inside a circular microchannel in the presence of a magnetic field. *International Journal of Thermal Sciences* 84, 196-206.

Malvandi, A. and D. D. Ganji (2014). Effects of nanoparticle migration on force convection of alumina/water nanofluid in a cooled parallel-plate channel. *Advanced Powder Technology* 25(4), 1369-1375.

Malvandi, A. and D. D. Ganji (2014). Magnetic field effect on nanoparticles migration and heat transfer of water/alumina nanofluid in a channel. *Journal of Magnetism and Magnetic Materials* 362(0), 172-179.

Malvandi, A. and D. D. Ganji (2014). Mixed convective heat transfer of water/alumina nanofluid inside a vertical microchannel. *Powder Technology* 263(0), 37-44.

Malvandi, A. and D. D. Ganji (2015). Effects of nanoparticle migration and asymmetric heating on magnetohydrodynamic forced convection of alumina/water nanofluid in microchannels. *European Journal of Mechanics - B/Fluids* 52, 169-184

Malvandi, A. and D. D. Ganji (2015). Effects of nanoparticle migration on hydromagnetic mixed convection of alumina/water nanofluid in vertical channels with asymmetric heating. *Physica E: Low-dimensional Systems and Nanostructures* 66, 181-196

Malvandi, A. and D. D. Ganji (2015). Magnetic field and slip effects on free convection inside a vertical enclosure filled with alumina/water nanofluid. *Chemical Engineering Research and Design* 94, 355-364

Malvandi, A., F. Hedayati and D. D. Ganji (2013). Thermodynamic optimization of fluid flow over an isothermal moving plate. *Alexandria Engineering Journal* 52(3), 277-283.

Malvandi, A., F. Hedayati and D. D. Ganji (2014). Slip effects on unsteady stagnation point flow of a nanofluid over a stretching sheet. *Powder Technology* 253, 377-384.

Malvandi, A., F. Hedayati, D. Ganji and Y. Rostamiyan (2014). Unsteady boundary layer flow of nanofluid past a permeable stretching/shrinking sheet with convective heat transfer. *Proceedings of the Institution of Mechanical Engineers, Part C: Journal of Mechanical Engineering Science* 228(7), 1175-1184.

Malvandi, A., M. H. Kaffash and D. D. Ganji (2015). Nanoparticles migration effects on magnetohydrodynamic (MHD) laminar mixed convection of alumina/water nanofluid inside microchannels. *Journal of the Taiwan Institute of Chemical Engineers* 52, 40-56.

Malvandi, A., M. R. Safaei, M. H. Kaffash and D. D. Ganji (2015). MHD mixed convection in a vertical annulus filled with Al2O3–water nanofluid considering nanoparticle migration. *Journal of Magnetism and Magnetic Materials* 382, 296-306.

Malvandi, A., S. A. Moshizi and D. D. Ganji (2014). Effect of magnetic fields on heat convection inside a concentric annulus filled with Al2O3–water nanofluid. *Advanced Powder Technology* 25(6), 1817-1824.

Malvandi, A., S. A. Moshizi, E. G. Soltani and D. D. Ganji (2014). Modified Buongiorno's model for fully developed mixed convection flow of nanofluids in a vertical annular pipe. *Computers and Fluids* 89(0), 124-132.

Masuda, H., A. Ebata, K. Teramae and N. Hishinuma (1993). Alteration of thermalconductivity and viscosity of liquid by dispersing ultra-fine particles. *Netsu Bussei* 7(4).

Maxwell, J. C. (1873). A Treatise on Electricity and Magnetism. Oxford, Uk, Clarendon press

Moshizi, S. A., A. Malvandi, D. D. Ganji and I. Pop (2014). A two-phase theoretical study of Al2O3–water nanofluid flow inside a concentric pipe with heat generation/ absorption. *International Journal of Thermal Sciences* 84(0), 347-357.

Nobari, M. R. H. and A. Malvandi (2013). Torsion and curvature effects on fluid flow in a helical annulus. *International Journal of Non-Linear Mechanics* 57(0), 90-101.

Pak, B. C. and Y. I. Cho (1998). hydrodynamic and heat transfer study of dispersed fluids with submicron metallic oxide particles. *Experimental Heat Transfer* 11(2), 151-170.

Rashidi, M. M., E. Momoniat, M. Ferdows and A. Basiriparsa (2014). Lie Group Solution for Free Convective Flow of a Nanofluid Past a Chemically Reacting Horizontal Plate in a Porous Media. *Mathematical Problems in Engineering* 21.

Rashidi, M. M., N. Freidoonimehr, A. Hosseini, O. A. Bég and T. K. Hung (2014). Homotopy simulation of nanofluid dynamics from a non-linearly stretching isothermal permeable sheet with transpiration. *Meccanica* 49, 2, 469-482

Shamshirband, S., A. Malvandi, A. Karimipour, M. Goodarzi, M. Afrand, D. Petković, M. Dahari and N. Mahmoodian (2015). Performance investigation of micro- and nano-sized particle

erosion in a 90° elbow using an ANFIS model. *Powder Technology* 284, 336-343

Sheikholeslami, M., M. Gorji-Bandpy and S. Soleimani (2013). Two phase simulation of nanofluid flow and heat transfer using heatline analysis. *International Communications in Heat and Mass Transfer* 47(0), 73-81.

Sheikholeslami, M., M. Gorji-Bandpy, D. D. Ganji, P. Rana and S. Soleimani (2014). Magnetohydrodynamic free convection of Al2O3–water nanofluid considering Thermophoresis and Brownian motion effects. *Computers and Fluids* 94(0), 147-160.

Sheikholeslami, M., M. Gorji-Bandpy, I. Pop and S. Soleimani (2013). Numerical study of natural convection between a circular enclosure and a sinusoidal cylinder using control volume based finite element method. *International Journal of Thermal Sciences* 72(0), 147-158

Soleimani, S., M. Sheikholeslami, D. D. Ganji and M. Gorji-Bandpay (2012). Natural convection heat transfer in a nanofluid filled semi-annulus enclosure. *International Communications in Heat and Mass Transfer* 39(4), 565-574

Tzou, D. Y. (2008). Thermal instability of nanofluids in natural convection. *International Journal of Heat and Mass Transfer* 51(11–12), 2967-2979

Yadav, D., J. Lee and H. H. Cho (2015). Brinkman convection induced by purely internal heating in a rotating porous medium layer saturated by a nanofluid. *Powder Technology* 286, 592-601

Yadav, D., R. Bhargava and G. S. Agrawal (2012). Boundary and internal heat source effects on the onset of Darcy–Brinkman convection in a porous layer saturated by nanofluid. *International Journal of Thermal Sciences* 60, 244-254

Yadav, D., R. Bhargava and G. S. Agrawal (2013). Numerical solution of a thermal instability problem in a rotating nanofluid layer. *International Journal of Heat and Mass Transfer* 63, 313-322

Yang, C., W. Li and A. Nakayama (2013). Convective heat transfer of nanofluids in a concentric annulus. *International Journal of Thermal Sciences* 71(0), 249-257

Yang, C., W. Li, Y. Sano, M. Mochizuki and A. Nakayama (2013). On the Anomalous Convective Heat Transfer Enhancement in Nanofluids: A Theoretical Answer to the Nanofluids Controversy. *Journal of Heat Transfer* 135(5), 054504-054504